Supporting Information

DePas et al. 10.1073/pnas.1218703110

SI Text

SI Materials and Methods

Reagents. Catalase from bovine liver, H_2O_2, $FeCl_3$, tryptophan, 2-Nitrophenyl β-D-galactopyranoside (ONPG), and $MnCl_2{\cdot}4H_2O$ were obtained from Sigma-Aldrich. Congo red (CR) was obtained from Acros Organics. Casamino acids were obtained from Amresco. Chelex-100 was obtained from Bio-Rad. Noble agar was obtained from BD. ProLong Gold Antifade Reagent was obtained from Invitrogen, and $CaCl_2$, $MgCl_2$, IPTG, tryptone, yeast extract, LB broth, Na_2CO_3, and agar were obtained from Fisher.

Strains and Cloning. UTI89 was obtained from Scott Hultgren (Washington University in St. Louis, St. Louis) (1). *Salmonella enterica* serovar *Typhimurium* strain ATCC 14028 was obtained from the American Type Tissue Collection. *Citrobacter koseri* was obtained from the University of Michigan Medical School. Strains were routinely grown in LB at 37 °C under aeration. The *sodA sodB* and *fur* mutants were grown without shaking to avoid excessive oxygen exposure. Mutations were introduced into UTI89 by the lambda Red recombinase method as described (2). The plasmid pCKR101 (3) was used for all overexpression experiments. For construction of overexpression vectors, inserts were amplified by PCR and cloned into the pCKR101 vector using KpnI and XbaI restriction sites. The *lacZ* transcriptional fusion plasmids pRJ800 (empty vector), pBA14 (*csgBAC* promoter driving *lacZ*), and pD1 (*csgDEFG* promoter driving *lacZ*) have been described (4). pRJ800-*adrA* (*adrA* promoter driving *lacZ*) was constructed by cloning a UTI89 genomic fragment including the *adrA* promoter into pRJ800 using BamHI and XbaI. Integration of the *csgBAC-mCherry* transcriptional fusion into the UTI89 *attB* site was performed as described (5, 6), except that *mCherry* was cloned from pAH6 (7) into pCD13psk using SpeI and SacI restriction sites, and the *csgBAC* promoter was cloned into pCD13psk from the UTI89 genome using HindIII and SpeI.

Rugose Formation and Low-Iron Media. For rugose biofilm development, UTI89 was grown overnight in LB, diluted to 1 OD_{600}, and rinsed twice with YESCA media (10 g Casamino acids, 1 g yeast extract/L). A 4-μL drop of a 1 OD_{600} cell mixture was spotted onto YESCA agar plates (10 g Casamino acids, 1 g yeast extract, 20 g agar/L). CR YESCA plates included a 50-μg/mL supplement of CR. Bacteria were incubated at 26 °C for 48 h unless otherwise noted. Pictures were taken with either a Canon EOS Rebel XSi camera or a Leica MZ FLIII Stereo-Fluorescence Microscope coupled to a Leica DC480 Microscope camera. For low-iron media, YESCA media was incubated with Chelex-100 at 5 g/100 mL for 2 h at room temperature with fresh resin or overnight (ON) at room temp with regenerated resin. Media was then filtered with 0.22-μM polyethersulfone (PES) bottle-top filters to separate the resin. For Chelex-treated agar plates, media was autoclaved with 1.4% Difco Noble Agar and supplemented with 100 μM $MgCl_2$, 10 μM $CaCl_2$, and 100 μM tryptophan. $FeCl_3$, $MnCl_2$, and IPTG were also supplemented where indicated. For typical rugose biofilm formation on Chelex-treated plates, cells were grown ON in LB, rinsed twice with Chelex-treated YESCA media, and resuspended at 1 OD_{600}. A total of 0 μL or 2 μL of 100 mM $FeCl_3$ (low-iron vs. high-iron conditions) was added to 100 μL of 1 OD_{600} cells. The 4-μL dots of these mixes were plated on Chelex-treated plates. For paper disk assays, 5 μL of indicated chemicals was added to sterile paper discs after cell mixes had been plated and had dried. For overexpression assays, IPTG was added to plates at a final concentration of 10 μM or 50 μM as noted. Ampicillin and kanamycin were added when appropriate to final concentrations of 100 μg/mL and 50 μg/mL, respectively. For rugose biofilm development, *S. typhimurium* was grown on LB–salt agar plates (10 g tryptone, 5 g yeast extract, 17 g agar /L) or Chelex-treated LB–salt agar plates for 72 h, and *C. koseri* was grown on YESCA agar plates or Chelex-treated YESCA agar plates for 48 h.

Confocal Microscopy. A 4-μL drop of 1 OD_{600} cells was dotted onto 0.05-μM MF-Millipore Membrane Filters that had been placed on YESCA agar plates or Chelex-treated YESCA plates. For induction of the pCKR101-*eGFP* or pCKR101-*mCherry* plasmids, 1 mM IPTG was added to cell mixtures before plating. After 48 h at 26 °C, colonies and their underlying filter were cut out with a razorblade and transferred to a microscope slide. A total of 100 μL of Invitrogen ProLongGold antifade reagent was added to the top of each biofilm, and a Fisherbrand No. 1.5, 24 × 60 mm coverslip was placed on top. Small spacers ∼0.3 mm in height were placed in each corner of the slide before addition of the coverslip to prevent direct contact between the biofilm and the coverslip. Samples were analyzed the next day with a Leica SP5 laser scanning confocal microscope on a DM6000B microscope base using a 20× or 40× objective. A double-dichroic 488/561 beam splitter and a 488-nm argon laser (eGFP) and a 561-nm diode-pumped solid-state laser (mCherry) were used for image capture. Images and movies were analyzed with LAS AF v2.6.3 build 8173 software.

H_2O_2 Viability Assays. For UTI89, mature biofilms or washout/matrix fractions were suspended in 50 mM KPi (pH 7.2) and tissue homogenized; 250 μL of cells normalized to 1 OD_{600} were then mixed with 250 μL 1% (vol/vol) H_2O_2 in 50 mM KPi (pH 7.2). This mixture was incubated for 20 min. A total of 500 μL of 1-mg/mL catalase was then added to stop H_2O_2-induced killing, and cells were spun down at 13,400 × *g* for 1 min. Cells were then resuspended in 250 μL 50-mM KPi (pH 7.2), and 4-μL dots of 10-fold serial dilutions were plated on LB plates and grown ON at 37 °C. *S. typhimurium* and *C. koseri* viability assays were performed identically, except that *S. typhimurium* was mixed with 1% (vol/vol) H_2O_2 for 15 min and *C. koseri* was mixed with 3% (vol/vol) H_2O_2 for 20 min.

Western Blot Analysis. Western blotting was performed as described (8) with modifications. Briefly, samples were treated with hexafluoroisopropanol (HFIP) to solubilize CsgA. After HFIP was removed with a Thermo Savant SPD SpeedVac, samples were resuspended in SDS running buffer. Samples were then electrophoresed in 15% polyacrylamide gels and transferred onto a nitrocellulose membrane in a wet transfer apparatus in 25 mM CAPS transfer buffer (pH 11.2) with 10% methanol. Blots were blocked with 5% milk in TBST for 1 h at room temp or ON at 4 °C. After TBST washes, blots were incubated for 1 h with primary (1:5,000 Santa Cruz RNA pol σ D antibody and 1:8,500 anti-CsgA peptide antibody) (4) and secondary (HRP-linked anti-mouse and anti-rabbit, both at 1:8,500) antibodies in 1% BSA, 1% milk in TBST at room temperature.

Oxygen Microelectrode Measurements. UTI89 was grown on YESCA agar plates for rugose biofilm formation. Oxygen microsensor measurements were performed as described (9, 10). All microprofiles were performed using Clark-type oxygen microelectrodes with outside tip diameters of 10 μm, response time 1–3 s, and <2% stirring sensitivity (Unisense, A/S). Amplification

and sensor positioning was controlled with a microsensor multimeter coupled with a motor-controlled micromanipulator. Data collection was aided by software SensorTrace Pro ver.3.0.1 (Unisense, A/S). Two-point calibrations were performed in air-saturated deionized (DI) water and in a 1 M NaOH/0.1 M ascorbic acid solution (anoxic standard). Calibrations were repeatedly checked in the anoxic standard and in air-saturated DI water throughout the experiments. Triplicate oxygen measurements (both biological and technical-position replicates) were done in one dimension (depth-wise) from the biofilm–air interface down in. The step size between measurements was 10 μm.

Quantitative Congo Red Binding. CR binding assays were performed as described (11) with modifications. Mature biofilms were harvested and suspended in 50 mM KPi (pH 7.2). A 300-μL suspension of 2 OD_{600} cells and 5 μg/mL CR was incubated with shaking at 37 °C for 30 min. Cells were then pelleted at 13,400 × *g* for 1 min, and 100 μL of the supernatant was assayed for absorbance at 490 nm in a Tecan Infinite M200 plate reader. Absorbances were then subtracted from a CR-only negative control, and percentage of CR removal was calculated, with the CR-only control representing 0% removed and the KPi-only control representing 100% removed. Error bars represent the SD of three biological replicates.

β-Galactosidase Assays. β-Galactosidase assays were performed as described (4, 12) with modifications. After 48 h of growth, a total of 100 μL of cells suspended in 50 mM KPi (pH 7.2) were added to the wells of a 96-well plate, and 7 μL were added to 90 μL reaction buffer. These reactions were incubated at 30 °C for 20 min before addition of 20 μL of 4 mg/mL ONPG. Reactions were stopped via addition of 50 μL 1 M Na_2CO_3 at a light yellow color, and the time was recorded. Absorbance of each cell suspension at 600 nm and absorbance of each reaction mixture at 420 nm and 550 nm were measured using a Tecan Infinite M200 plate reader. β-Galactosidase assays were performed in triplicate on a strain carrying an empty vector (pRJ800) under each condition. Average Miller units from the pRJ800-carrying strains were subtracted from values obtained from each respective strain carrying pBA14, pD1, or pRJ800-*adrA*. After subtracting out the empty-vector values, averages, SDs, and *P* values were calculated from biological triplicates of strains carrying pBA14, pD1, or pRJ800-*adrA* as noted.

1. Mulvey MA, Schilling JD, Hultgren SJ (2001) Establishment of a persistent *Escherichia coli* reservoir during the acute phase of a bladder infection. *Infect Immun* 69(7): 4572–4579.
2. Datsenko KA, Wanner BL (2000) One-step inactivation of chromosomal genes in *Escherichia coli* K-12 using PCR products. *Proc Natl Acad Sci USA* 97(12): 6640–6645.
3. Keyer K, Imlay JA (1996) Superoxide accelerates DNA damage by elevating free-iron levels. *Proc Natl Acad Sci USA* 93(24):13635–13640.
4. Barnhart MM, Lynem J, Chapman MR (2006) GlcNAc-6P levels modulate the expression of Curli fibers by *Escherichia coli*. *J Bacteriol* 188(14):5212–5219.
5. Platt R, Drescher C, Park SK, Phillips GJ (2000) Genetic system for reversible integration of DNA constructs and lacZ gene fusions into the *Escherichia coli* chromosome. *Plasmid* 43(1):12–23.
6. Wright KJ, Seed PC, Hultgren SJ (2005) Uropathogenic *Escherichia coli* flagella aid in efficient urinary tract colonization. *Infect Immun* 73(11):7657–7668.
7. Lauderdale KJ, Boles BR, Cheung AL, Horswill AR (2009) Interconnections between Sigma B, agr, and proteolytic activity in *Staphylococcus aureus* biofilm maturation. *Infect Immun* 77(4):1623–1635.
8. Zhou Y, Blanco LP, Smith DR, Chapman MR (2012) Bacterial amyloids. *Methods Mol Biol* 849:303–320.
9. Rani SA, et al. (2007) Spatial patterns of DNA replication, protein synthesis, and oxygen concentration within bacterial biofilms reveal diverse physiological states. *J Bacteriol* 189(11):4223–4233.
10. Revsbech NP (1989) An oxygen microsensor with a guard cathode. *Limnol Oceanogr* 34(2):474–478.
11. Ma Q, Wood TK (2009) OmpA influences *Escherichia coli* biofilm formation by repressing cellulose production through the CpxRA two-component system. *Environ Microbiol* 11(10):2735–2746.
12. Miller JH (1972) *Experiments in molecular genetics* (Cold Spring Harbor Lab Press, Cold Spring Harbor, NY).

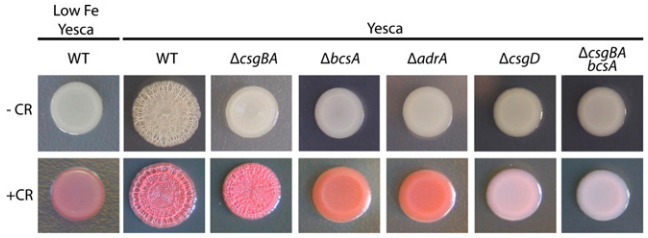

Fig. S1. WT UTI89 and mutants were plated on YESCA agar plates or Chelex-treated YESCA agar plates with or without the addition of CR. Strains producing either curli or cellulose bind CR, but a curli cellulose double mutant (*csgBA bcsA*) does not. A *csgD* mutant does not bind CR, indicating that CsgD is required for curli and cellulose production in UTI89. Both curli and cellulose are required for WT rugose biofilm formation.

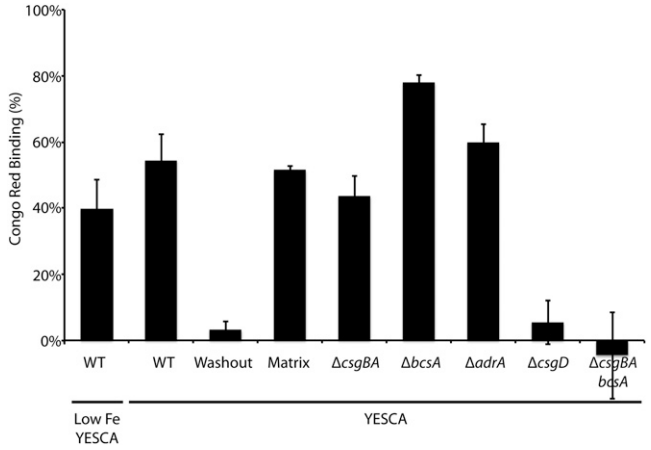

Fig. S2. Suspended bacteria were incubated with 5 μg/mL CR in KPi buffer, spun out of suspension, and the percent of CR taken out of solution by the bacteria was assayed by absorbance at 490 nm of the supernatant. A CR-only control represents 0% CR binding, and a KPi-only control represents 100% CR binding. Error bars represent the SD of biological triplicates.

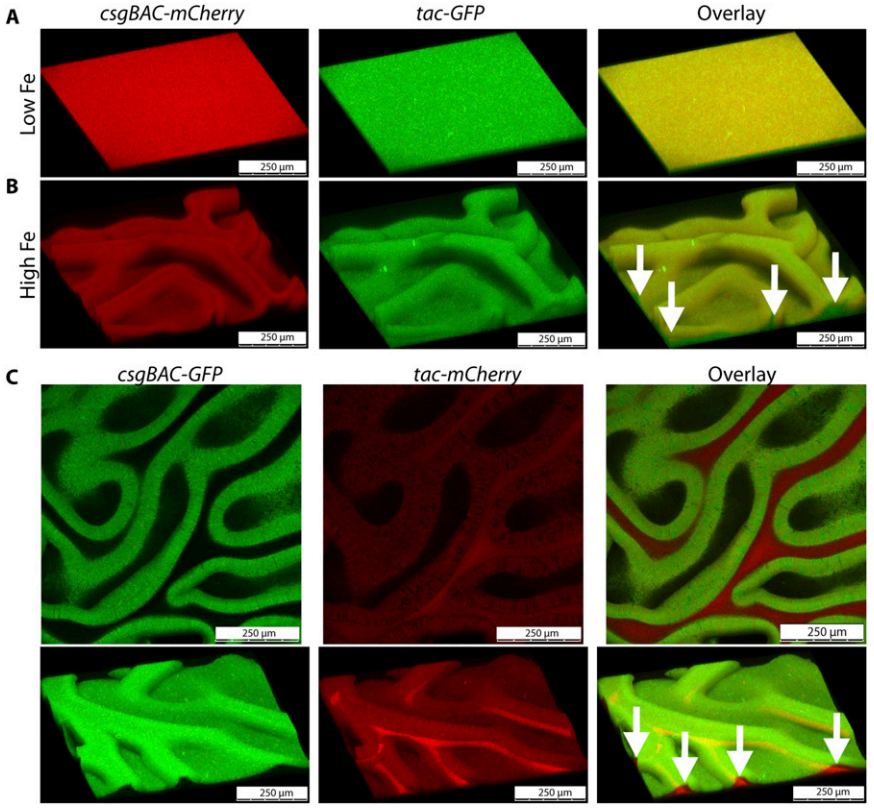

Fig. S3. (*A*) UTI89 *attB*::*csgBAC-mCherry*/pCKR101-*eGFP* was grown on Chelex-treated YESCA plates on a cellulose filter and visualized by confocal microscopy, revealing little spatial separation of curli-producing and non–curli-producing bacteria. (*B*) UTI89 *attB*::*csgBAC-mCherry*/pCKR101-*eGFP* with $FeCl_3$ added back to the cell mixture before plating on Chelex-treated YESCA plates demonstrates identical architecture as the same strain grown on YESCA plates. (*C*) A UTI89 *attB*::*csgBAC-eGFP*/pCKR101-*mCherry* strain grown on a YESCA plate demonstrates mCherry-producing cells lining the interior of mCherry/GFP-expressing surface bacteria. White arrows indicate sites where non–curli-producing bacteria can be seen in wrinkle interiors.

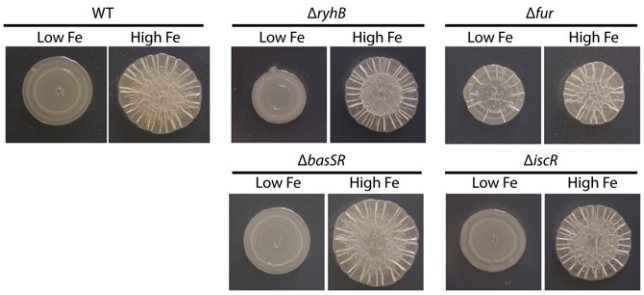

Fig. S4. WT UTI89 as well as *iscR*, *basSR*, *fur*, and *ryhB* mutants were plated on Chelex-treated YESCA agar plates with or without addition of $FeCl_3$ to the cell mixture before plating. Only the *fur* mutant demonstrated an increase in rugose biofilm formation in low-iron conditions.

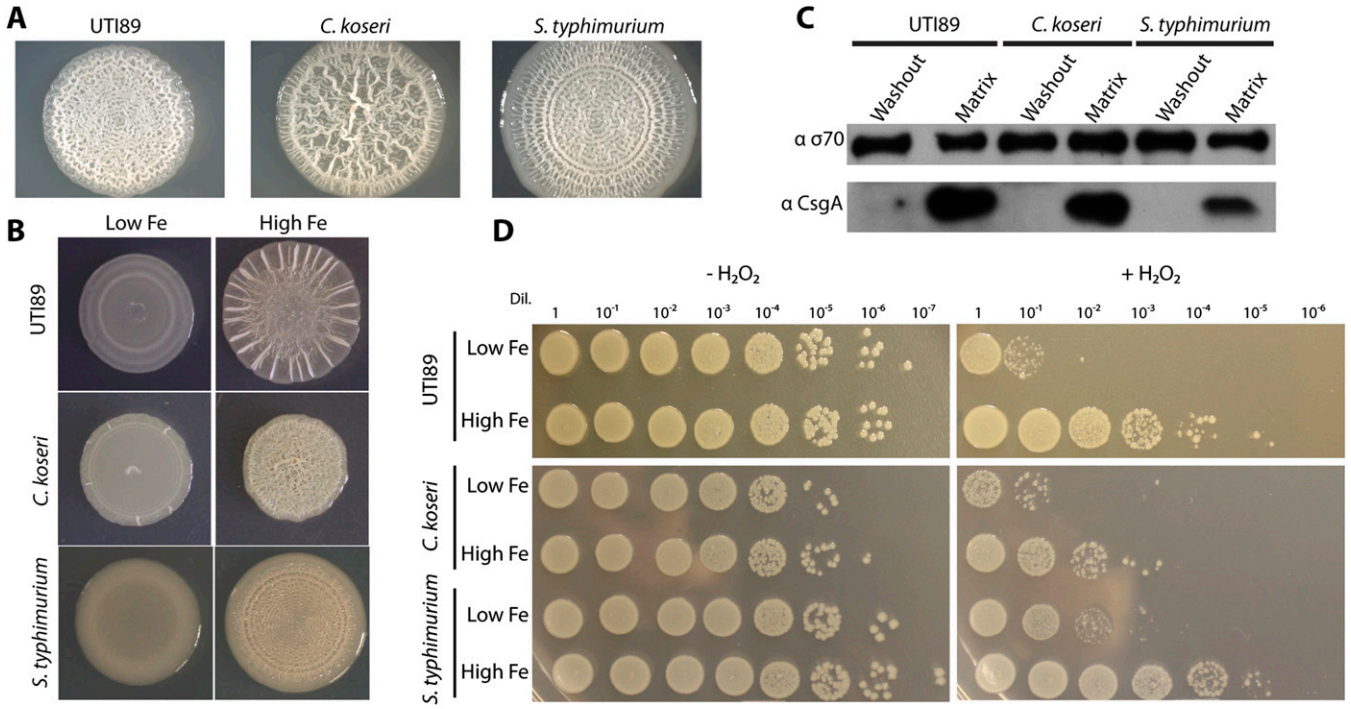

Fig. S5. (*A*) UTI89 and *C. koseri* form rugose biofilms on YESCA plates after 48 h, and *S. typhimurium* forms rugose biofilms on LB–salt agar plates after 72 h. (*B*) Iron is required for rugose biofilm formation of UTI89 and *C. koseri* on Chelex-treated YESCA plates and for S. *typhimurium* on Chelex-treated LB–salt plates. (*C*) Whole-cell Western blot analysis performed on washout and matrix fractions demonstrates that CsgA is chiefly localized to the matrix fraction in all three strains. (*D*) When grown in low-iron conditions, all three strains were more susceptible to H_2O_2 treatment than after growth in high-iron conditions. UTI89 was mixed with 1% (vol/vol) H_20_2 for 20 min as described in *Materials and Methods*, *C. koseri* was mixed with 3% (vol/vol) H_20_2 for 20 min, and *S. typhimurium* was mixed with 1% (vol/vol) H_20_2 for 15 min.

Table S1. Strains and plasmids used in this study

	Source	Notes
Plasmid		
pCKR101	(1)	
pCKR101-*sodA*	This work	*sodA* cloned into KpnI and XbaI sites of pCKR101 with primers WD229 and WD209 from UTI89 genome
pCKR101-*eGFP*	This work	*eGFP* cloned into KpnI and XbaI sites of pCKR101 with primers WD263 and WD264 from genome of UTI89 attB::*csgBAC-eGFP*
pCKR101-*mCherry*	This work	*mCherry* cloned into KpnI and XbaI sites of pCKR101 with primers WD244 and WD245 from pAH6
pRJ800	(2)	*lacZ*-expressing plasmid with no promoter sequence, used as empty vector for β-galactosidase assays
pBA14	(2)	*csgBAC* promoter driving *lacZ* in pRJ800 vector
pD1	(2)	*csgDEFG* promoter driving *lacZ* in pRJ800 vector
pRJ800-*adrA*	This work	*adrA* promoter cloned into BamHI and XbaI sites of pRJ800 with primers DH1 and DH2 from the UTI89 genome
pAH6	(3)	
pCD13psk	(4, 5)	
pCD13psk-*mCherry*	This work	*mCherry* cloned from pAH6 into pCD13psk SpeI and SacI sites using primers WD119 and WD120
pCD13psk-*csgBAC-mcherry*	This work	UTI89 *csgBAC* promoter from the UTI89 genome cloned into pCD13psk-*mcherry* HindIII and SpeI sites using primers WD214 and WD215
Strain		
UTI89	(6)	
C. koseri	Isolate from University of Michigan Medical School	
Salmonella enterica serovar *typhimurium* ATCC 14028	ATCC	
UTI89 *csgBA*::kan	This work	Red swap mutagenesis of WT UTI89 with primers WD6 and WD7
UTI89 *csgD*::kan	This work	Red swap mutagenesis of WT UTI89 with primers WD36 and WD37
UTI89 *bcsA*::kan	This work	Red swap mutagenesis of WT UTI89 with primers WD349 and WD350
UTI89 *adrA*::kan	This work	Red swap mutagenesis of WT UTI89 with primers WD99 and WD100
UTI89 *attB*::*csgBAC-mCherry*	This work	As described (7), except *mCherry* was cloned from pAH6 into pCD13psk using primers WD119 and WD120
UTI89 *attB*::*csgBAC-mCherry*/pCKR101-*eGFP*	This work	UTI89 *attB*::*csgBAC-mCherry* electroporated with pCKR101-*eGFP*
UTI89 *attB*::*csgBAC-eGFP*	(7)	
UTI89 *attB*::*csgBAC-eGFP*/pCKR101-*mCherry*	This work	UTI89 *attB*::*csgBAC-eGFP* electroporated with pCKR101-*mCherry*
UTI89 *sodA*::kan	This work	Red swap mutagenesis of WT UTI89 with primers WD202 and WD203
UTI89 *sodA*::flp *sodB*::kan	This work	Red swap mutagenesis of UTI89 *sodA*::flp with primers WD239 and WD240
UTI89 *fur*::kan	This work	Red swap mutagenesis of WT UTI89 with primers WD15 and WD17
UTI89 *iscR*::kan	This work	Red swap mutagenesis of WT UTI89 with primers WD18 and WD19
UTI89 *ryhB*::kan	This work	Red swap mutagenesis of WT UTI89 with primers WD297 and WD79
UTI89 *basSR*::kan	This work	Red swap mutagenesis of WT UTI89 with primers WD221 and WD252
UTI89/pCKR101	This work	UTI89 electroporated with pCKR101
UTI89/pCKR101-*sodA*	This work	UTI89 electroporated with pCKR101-*sodA*
UTI89 *sodA*::flp *sodB*::kan/pCKR101	This work	UTI89 *sodA*::flp *sodB*::kan electroporated with pCKR101
UTI89 *sodA*::flp *sodB*::flp/pCKR101-*sodA*	This work	UTI89 *sodA*::flp *sodB*::flp electroporated with pCKR101-*sodA*
UTI89 *fur*::kan/pCKR101	This work	UTI89 *fur*::kan electroporated with pCKR101
UTI89 *fur*::kan/pCKR101-*sodA*	This work	UTI89 *fur*::kan electroporated with pCKR101-*sodA*

1. Keyer K, Imlay JA (1996) Superoxide accelerates DNA damage by elevating free-iron levels. *Proc Natl Acad Sci USA* 93(24):13635–13640.
2. Barnhart MM, Lynem J, Chapman MR (2006) GlcNAc-6P levels modulate the expression of Curli fibers by *Escherichia coli*. *J Bacteriol* 188(14):5212–5219.
3. Lauderdale KJ, Boles BR, Cheung AL, Horswill AR (2009) Interconnections between Sigma B, agr, and proteolytic activity in *Staphylococcus aureus* biofilm maturation. *Infect Immun* 77(4):1623–1635.
4. Platt R, Drescher C, Park SK, Phillips GJ (2000) Genetic system for reversible integration of DNA constructs and lacZ gene fusions into the *Escherichia coli* chromosome. *Plasmid* 43(1): 12–23.
5. Wright KJ, Seed PC, Hultgren SJ (2005) Uropathogenic *Escherichia coli* flagella aid in efficient urinary tract colonization. *Infect Immun* 73(11):7657–7668.
6. Mulvey MA, Schilling JD, Hultgren SJ (2001) Establishment of a persistent *Escherichia coli* reservoir during the acute phase of a bladder infection. *Infect Immun* 69(7):4572–4579.
7. Cegelski L, et al. (2009) Small-molecule inhibitors target *Escherichia coli* amyloid biogenesis and biofilm formation. *Nat Chem Biol* 5(12):913–919.

Table S2. Primers used in this study

Primer	Sequence
WD6	5′ AAATACAGGTTGCGTTAACAACCAAGTTGAAATGATTTAATTTCT TAAGTGTGTAGGCTGGAGCTGCTT 3′
WD7	5′ CGAAAAAAAACAGGGCTTGCGCCCTGTTTCTTTAATACAGAGGA TGTATATGAATATCCTCCTTAG 3′
WD15	5′ CACTTCTAATGAAGTGAACCGCTTAGTAACAGGACAGATTCCGC ATGATTCCGGGGATCCGTCGACC 3′
WD17	5′ GCAGGTTGGCTTTTCTCGTTCAGGCTGGCTTATTTGCCTTCGTGCGC GTGTGTAGGCTGGAGCTGCTTCG 3′
WD18	5′ TACAATAAAAAACCCCGGGCAGGGGCGAGTTTGAGGTGAAGTAA GACATGATTCCGGGGATCCGTCGACC 3′
WD19	5′ CACTCCGGCCTGATTCTGAATTCTTTTTATTAAGCGCGTAACTTAACG TCTGTAGGCTGGAGCTGCTTCG 3′
WD36	5′ CAATCCAGCGTAAATAACGTTTCATGGCTTTATCGCCTGAGGTTATCG TTCATATGAATATCCTCCTTA 3′
WD37	5′ GAGGCAGCTGTCAGGTGTGCGATCAATAAAAAAAGCGGGGTTTCATC ATGGTGTAGGCTGGAGCTGCTTC 3′
WD79	5′ TTTGCAAAAAGTGTTGGACAAGTGCGAATGAGAATGATTATTATTGT CTCGCGGTGTAGGCTGGAGCTGCTTC 3′
WD99	5′ CTTCTGCCTTTAGCCCCGTCTCTATAATTTGGGAAAATTGTTTCTGAATGGTGTA GGCTGGAGCTGCTTC 3′
WD100	5′ CAGCAAATCCTGATGGCTTTTGCCGGACGTCAGGCCGCCACTTCGGTGCGCATATGAAT ATCCTCCTTAG 3′
WD119	5′ gatcactagtATGGTGAGCAAGGGCGAGGAGGATA 3′
WD120	5′ gatcgagctcCTACTTGTACAGCTCGTCCATGCCG 3′
WD202	5′ AACGCCTCATTGCAGCAGGCATCAAATGATTATTTTTTCGCTGCGAAAC GGTGTAGGCTGGAGCTGCTTC 3′
WD203	5′ CTTACGCGGCATTAACAATCGGCCGCCCGACAACACTGGAGATGAATAT GCATATGAATATCCTCCTTAG 3′
WD209	5′ gatctctagaTTATTTTTTCGCTGCGAAACGTGCC 3′
WD214	5′ gatcaagcttGTTTTTCCTGCTCAAAGTATCC 3′
WD215	5′ gatcactagtTGCGCAACAACCGCCAAAAG 3′
WD221	5′ TACCAGGCTGCGGATGATATTCTGCAAACTTGCAGGAGAGTGAGTGAA TGGTGTAGGCTGGAGCTGCTTC 3′
WD229	5′ gatcggtaccGCCGCCCGACAACACTGGAGATG 3′
WD239	5′ AATAAGGCTATTGTACGTATGCAAATTAATAATAAAGGAGAGTAGCA ATGGTGTAGGCTGGAGCTGCTTC 3′
WD240	5′ TCAGATAATGTTGCATTTGCCATCAGTTATTATGCAGCGAGATTTTTCGC CATATGAATATCCTCCTTAG 3′
WD244	5′ gatcggtaccTAGGGAGGTTTTAAACATGGTGAGC 3′
WD245	5′ gatctctagaTTACTTGTACAGCTCGTCCATGCC 3′
WD252	5′ TTCAGCGTGCTGGTGGTCAGCAGCTTTCTTTATATCTGGTTTGCCACGTACATATGA ATATCCTCCTTAG 3′
WD263	5′ gatcggtaccGGTACCTAGAATTAAAGAGGAGAAA 3′
WD264	5′ gatctctagaTTATTTGTATAGTTCATCCATGCCA 3′
WD297	5′ AACGAACACAAGCACTTCCCGAGGATAAATTGAGAACGAAAGGTCAAAAAAAAC ATATGAATATCCTCCTTAG 3′
WD349	5′ TGCCTGTTAAACTATTCCGGGCTGAAAATGCCAGTCGGGAGTGCATCATGCATA TGAATATCCTCCTTAG 3′
WD350	5′ AGAATATTTTTCTTTTCATCGCGTTATCATCATTGTTGAGCCAAAGCCTGGTGT AGGCTGGAGCTGCTTC 3′
DH1	5′ gatcggatccCAAAAGATGCGCGAATGTAATAATC 3′
DH2	5′ gatctctagaTCAGAAACAATTTTCCCAAATTATA 3′

Noncomplementary regions are lowercased.

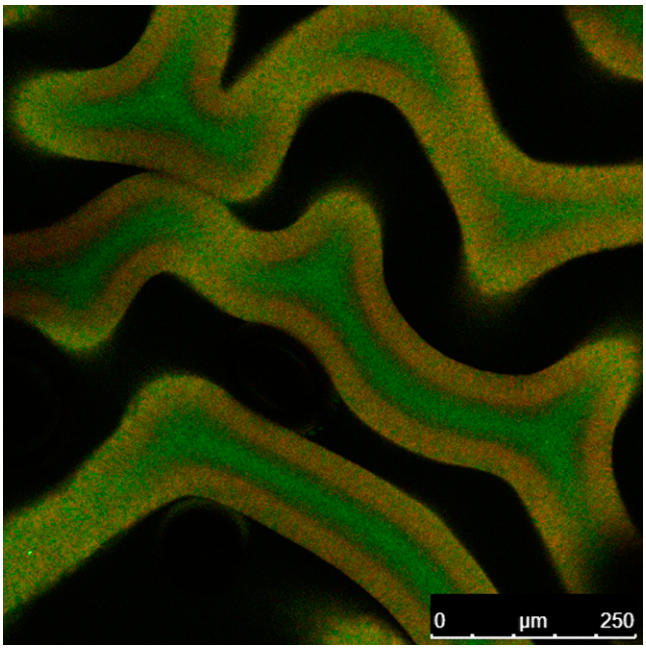

Movie S1. Z-stack of UTI89 *attB*::*csgBAC-mCherry*/pCKR101-e*GFP* grown on a YESCA agar plate on top of a 0.05-μm cellulose filter. All metabolically active bacteria are producing GFP, whereas curli-producing cells are producing both mCherry and GFP. Confocal microscopy was performed as described in *Materials and Methods*. Video starts from the bottom (agar surface) and moves through the top (air–biofilm interface). GFP-producing cells line the interior of the wrinkles, whereas GFP/mCherry-producing cells coat the biofilm surface.

Movie S1

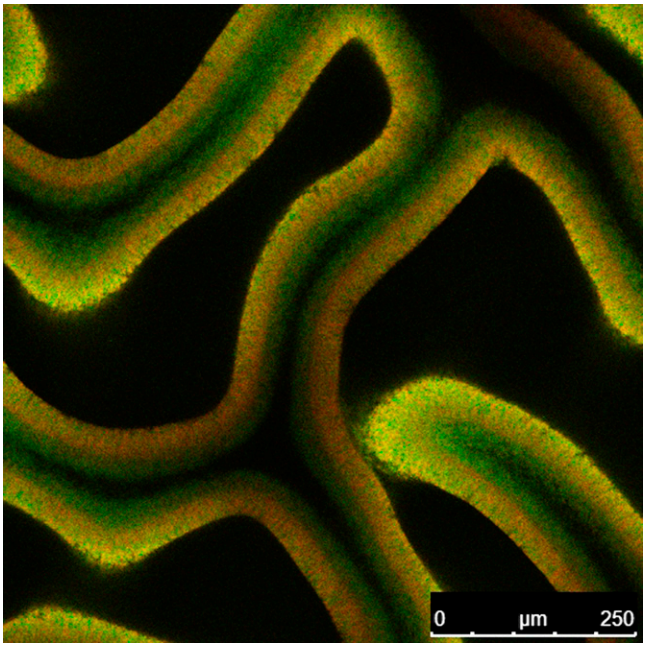

Movie S2. Z-stack of UTI89 *attB*::*csgBAC-mCherry*/pCKR101-e*GFP* grown on a YESCA agar plate on top of a 0.05-μm cellulose filter. The washout assay was performed, and afterward the matrix fraction was positioned onto the cellulose filter and confocal microscopy was performed as described. All metabolically active bacteria are producing GFP, whereas curli-producing cells are producing both mCherry and GFP. Video starts from the bottom (agar surface) and moves through the top (air–biofilm interface). A majority of the non–curli-producing bacteria from the interior of the wrinkles were absent after the washout assay was performed.

Movie S2